Appl. Phys. B 55, 424–429 (1992)

Applied Physics B Photophysics and Laser Chemistry

OH Rotational Temperature and Number Density Measurements in High-Pressure Laminar Flames Using Double Phase-Conjugate Four-Wave Mixing

D. A. Feikema*, E. Domingues, and M.-J. Cottereau

URA CNRS 230/CORIA, B.P. 118, F-76134 Mont Saint Aignan Cedex, France (Fax: +33/35708384)

Received 3 June 1992/Accepted 23 July 1992

Abstract. OH number densities and rotational temperatures up to 9 bar have been measured using double-phase-conjugate four-wave mixing (DPCFWM) in flat laminar premixed methane/air flames. By phase conjugating the backward pump to the forward pump with a phase-conjugate mirror conventional degenerate four-wave mixing (DFWM) becomes DPCFWM and quantitative measurements of OH radicals and OH rotational temperatures in flames at high pressure are possible. Our results show that conventional DFWM with a standard mirror is a low-biased measurement at high pressure primarly due to a fluctuating interaction volume which results from large fluctuating density gradients at the edge of the flame and from flame movement. A comparison is made between a laser-saturated fluorescence technique, conventional DFWM, and DPCFWM at 1, 5 and 9 bar.

PACS: 42.65, 82.40

In the field of nonintrusive optical combustion diagnostics, advances in laser technology and electronics for spectroscopic measurements are helping to provide new data concerning molecular species important in hydrocarbon pollution chemistry as well as other important aspects of combustion science and technology. Also, combustion diagnostics are providing invaluable data in more practical turbulent combustion systems which is enhancing turbulent combustion modeling perspectives.

Linear optical diagnostics such as laser-induced fluorescence and absorption techniques are generally employed for detecting minor reactive species (OH, CH, CN, NH, NO). Nonlinear optical diagnostics have also proven very valuable. One such technique is coherent anti-Stokes Raman spectroscopy (CARS) which possesses the capability to measure temperature and major species concentrations even in hostile and optically remote environments. When the participating wave mixing laser beams are aligned with an electronic absorption transition, CARS becomes resonance CARS, which greatly increases the signal strength, however only at the expense of greater experimental complexity and spectral interpretation.

Degenerate four-wave mixing (DFWM) and CARS are closely related coherent nonlinear optical processes which rely on the third-order susceptibility. The DFWM technique and its variants have been successfully used in atmospheric and subatmospheric flames to date by some researchers [1–10]. Early theoretical treatments of DFWM can be found in [13, 15].

Recent investigations indicate, that DFWM can approach sensitivities of laser-induced fluorescence techniques and because of optical phase conjugation can be extended to two dimensions even in luminous combustion environments provided absorption is small.

In the present paper we report an extension of DFWM, namely, double phase-conjugate four-wave mixing (DPCFWM) for measurement of the OH molecule in high-pressure flat, laminar, premixed methane/air flames. Using the DPCFWM experimental setup [1, 2], measurements at high pressure, here up to 9 bar, become meaningful. The DPCFWM, DFWM, and a saturated laser-induced fluorescence technique are compared and we find that DPCFWM is very sensitive at high pressure and correctly phase conjugates the backward pump to the forward pump. Using this method a non-fluctuating interaction volume between forward and backward pumps and the probe can be achieved. This essentially eliminates the low-bias in the DFWM measurement and renders DPCFWM, which has all the advantageous characteristics of DFWM, applicable in more complicated high-pressure reacting flows such as rockets, engines, etc.

1 Experimental

Figure 1 shows the current experimental setup. A Quantel Datachrom multimode doubled Nd:YAG pumped dye

* *Present address:* University of Alabama, Propulsion Research Center, Huntsville, AL 35899, USA (Fax: +1-205/890-7205)

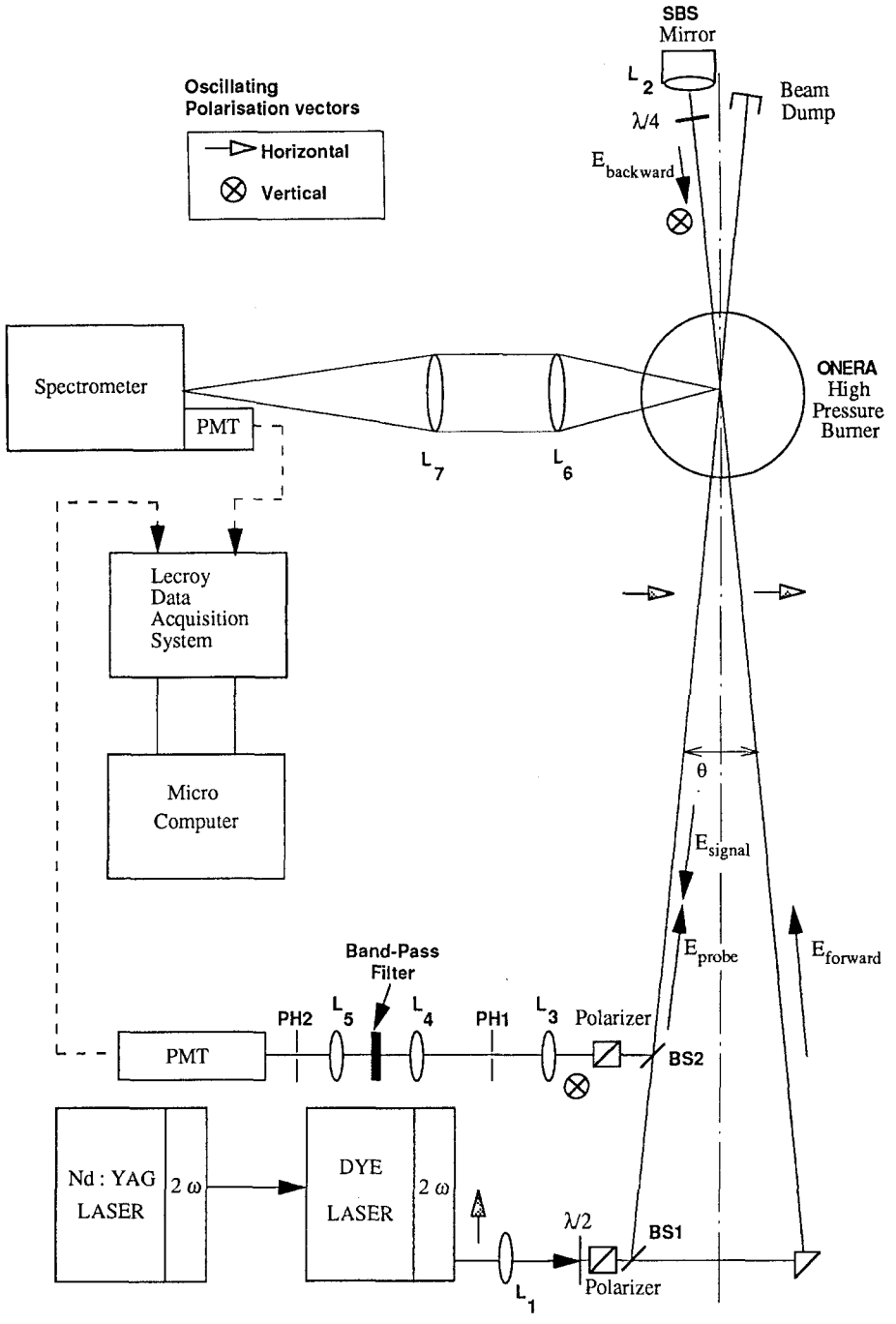

Fig. 1. Experimental setup: L1: ($f_L = 1500$ mm); L2: ($f_L = 7.5$ mm); L3: ($f_L = 40$ mm); L4: ($f_L = 250$ mm); L5: ($f_L = 150$ mm); L6: ($f_L = 200$ mm); L7: ($f_L = 200$ mm); BS1 and BS2 (beam splitter plates: transmission 70%, reflectivity 30%); PH1: (pin-hole 100 μm); PH2: (pin-hole 80 μm); $\theta = 4°$, $I_{Forward} = 1.3$ mJ/pulse; $I_{Backward} = 0.2$ mJ/pulse: $I_{probe} = 0.5$ mJ/pulse

laser was used with an approximate pulse duration of 10 ns, pulsing rate of 10 Hz, and a maximum energy of 18 mJ/pulse. Neutral density filters are used to lower the laser energy when performing experiments. A tracking system has been installed which tracks the dye laser's fundamental intensity and adjusts the second frequency-doubled crystal. This system enables absorption scans of the laser while maintaining approximately constant laser power. The FWHM linewidth of the laser in the ultraviolet was estimated by direct absorption measurement to be 0.7 cm^{-1} which has been estimated to be equal to the pressure broadened absorption line of the OH radical at 9 bar and therefore larger than the absorption line a 1 bar and at 5 bar [17]. Temperature regulation of the doubling generators and the dye cavity were required to prevent thermal instabilities and large fluctuations in laser power. At the exit of the dye laser in the ultraviolet near 306.6 nm the laser is focused by lens L1($f_L = 1500$ mm) into the ONERA high-pressure flat flame burner (see [11, 12] for details). The laser beam is horizontally polarized and is split using beam splitter BS1($T = 70\%$, $R = 30\%$). The forward pump and probe intersect inside the flat premixed flame at approximately $\theta = 4°$. The interaction length is approximately 20 mm and the focused laser beams are approximately 200 μm in diameter. The probe wave (0.5 mJ/pulse) is optically dumped for both the DFWM and DPCFWM methods. Using the DFWM arrangement a standard mirror reflects the forward pump to form the backward pump. In the DPCFWM arrangement the strong forward pump (1.3 mJ/pulse) is focused into

liquid hexane after passing through lens L2 ($f_L = 7.5$ mm). The stimulated Brillouin scattered (SBS) phase conjugate wave returns along the same optical path with inverse $\mathbf{K}_{\text{Forward}}$ vector and a quarter wave plate rotates the polarization vector relative to the forward pump by 90° (45° for each pass). The reflectivity of the SBS mirror is approximately 20%, thus the backward pump has about 0.2 mJ/pulse. The SBS phenomenon induced a frequency shift in the phase-conjugate pump wave relative to the forward pump which is given by [15]

$$\Delta\nu_{\text{SBS}} = 2\nu_{\text{Laser}}\sqrt{\frac{T}{\varrho}}\frac{n_{\text{Hexane}}}{c}, \tag{1}$$

where T is the bulk models of liquid hexane, (6.0×10^8 N/m^2) [16], ϱ is the density, n is the index of refraction, ν_{Laser} is the monochromatic laser frequency, and c is the speed of light. At atmospheric pressure and temperature a SBS frequency shift of 8 GHz is calculated. It is noted that this frequency shift, as calculated using (1), is smaller than our laser FWHM bandwidth of 20 GHz (0.7 cm^{-1}).

Because of the phase matching condition, the signal wave travels with inverse $\mathbf{K}_{\text{Signal}}$ vector to the probe and is collected after reflecting off a second beam splitter BS2 ($R = 30\%$, $T = 70\%$). A polarizer is aligned vertically so as to eliminate stray reflections from the quartz windows and linearly scattered light. The signal wave is focused and passed through two pinholes PH1 (100 μm) and PH2 (80 μm) to minimize noise.

The signal to noise ratio was measured to vary from as high as 200:1 to less than 1:1 depending on the OH number density, line strength, and method (i.e. DFWM or DPCFWM). A 200:1 ratio was measured with DFWM in a 1 bar, stoichiometric methane/air premixed flame 5 mm above the burner, where N_{OH} was measured by absorption to be 7.0×10^{15} OH molecules/cm^3. In this case the laser was tuned to the line $Q_1(13)$ of the $A^2\Pi(v'=0) \Leftarrow X^2\Sigma^+(v''=0)$ system of OH. For DPCFWM the signal to noise ratio is lower than for DFWM primarily because the backward pump is lower in power for DPCFWM. A signal to noise ratio of 50:1 was obtained in the same flame and on the same line as DFWM as described above. By increasing the reflectivity of the SBS mirror, the DPCFWM signal to noise ratios can be improved. When the OH number density was reduced to 1.0×10^{15} OH molecules/cm^3, DPCFWM signal to noise ratio of approximately 1:1 was obtained and thus this represents a limit of detectability for the present DPCFWM configuration using the $Q_1(13)$ line. However, to lower the limit of detectability a stronger line can be selected (i.e. $P_1(6)$ line of the $A^2\Pi(v'=0) \Leftarrow X^2\Sigma^+(v''=0)$ band of OH). Our results indicate the OH detectability is on the order of 2×10^{14} OH molecules/cm^3 for DFWM and 5×10^{14} OH molecules/cm^3 for higher than for fluorescence (i.e. 10^{13} OH molecules/cm^3).

For the measurements of OH number density (Figs. 2, 3; Tables 2, 3) the laser was tuned on the $Q_1(13)$ line of $A^2\Pi(v'=0) \Leftarrow X^2\Sigma^+(v''=0)$ band of OH and the fluorescence signal was detected on the $P_1(14)$ line of OH. The fluorescence optical path slices a vertical disk of the intersecting laser beams and is collected simultaneously with the DFWM and/or DPCFWM signals. The fluorescence light is focused onto the entrance slit of a Jobin Yvon spectrometer of 60 cm focal length. The fluorescence, DFWM, and DPCFWM signals are detected using photomultiplier tubes (model # XP 2020 RTC). A Lecroy CAMAC data acquisition system collects and stores two signals simultaneously shot by shot of the laser.

2 Results and Discussion

In the premixed flat flame high-pressure ONERA burner many flames have been studied and measured [11, 12]. For the present measurements a lean methane/air flame, $\phi = 0.85$, was selected since N_{OH} is relatively high and signals are very strong. Also, it was found, that for the $\phi = 0.85$ flame, inherent experimental fluctuations in N_{OH} due to fluctuations in fuel equivalence ratio were held to a minimum. The actual values of the flow rates used for the present experiments are provided in Table 1.

In Table 2 the root mean square fluctuations of the fluorescence, DFWM, and DPCFWM signals are tabulated for 1, 5, and 9 bar. The results show that at 1 bar the DFWM and fluorescence signals fluctuate less than the DPCFWM signal. With our experimental arrangement DFWM is a better technique at 1 bar than DPCFWM since signals fluctuate less. A possible explanation for this larger r.m.s. fluctuation could be that the intensity of the backward pump is stronger (i.e. 1.3 mJ/pulse) with the classical DFWM technique while for the DPCFWM technique the backward pump energy is 80% less and its energy fluctuates more than in the DFWM configuration. Another possible explanation could be attributed to the SBS frequency shift in the backward pump which is calculated to be 8 GHz. At 1 bar the FWHM linewidth of OH is also estimated to be 8 GHz [17]. This frequency shift in the backward pump creates a complicated phase

Table 1. Flow rates of air (actually: 80% N_2 and 20% O_2 by volume), methane, and coaxial nitrogen

Pressure [bar]	Air at STP [dm^3/min]	Methane, $\phi = 0.85$ [dm^3/min at STP]	Coaxial nitrogen [dm^3/min at STP]
1.0	4.2	0.36	4.0
5.0	8.4	0.71	36.0
9.0	13.0	1.11	43.0

Table 2. Root mean square signal fluctuations for fluorescence, DFWM, and DPCFWM signals at 1, 5, and 9 bar, 5 mm above the burner, and fuel equivalence ratio: $\phi = 0.85$

Pressure [bar]	Fluorescence	DFWM	DPCFWM
1.0	± 6%	± 9%	±18%
5.0	± 8%	± 45%[a]	±20%
9.0	±10%	±115%[a]	±27%

[a] Means low-biased non-Gaussian histogram (see Fig. 2)

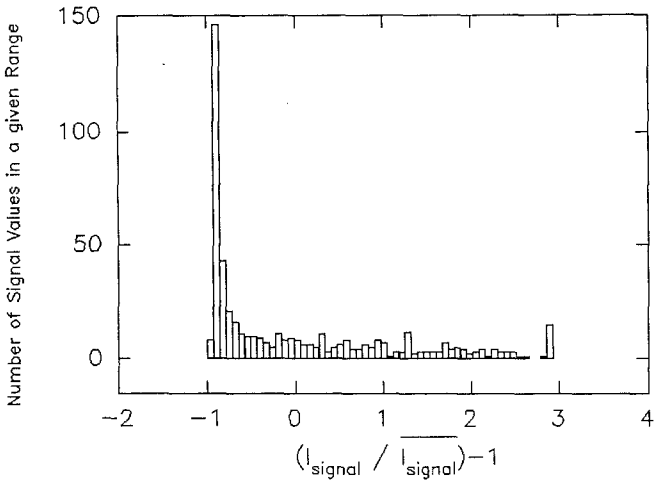

Fig. 2. Histogram of the DFWM signal based on 500 samples in a lean, $\phi=0.85$, methane/air laminar flame at 9 bar, at 5 mm above the burner

shift and potential spectral instabilities due to detuning the backward pump by $\Delta\nu_{SBS}$ to the probe and forward pump waves.

Figures 2 and 3 show the histograms for DFWM and DPCFWM, respectively, at 9 bar and represent the same data as given in Tables 2 and 3. The histograms are shown plotted as a function of $((I_{Signal}/\overline{I_{Signal}})-1.0)$. A value of zero corresponds to the mean signal value and a value of minus one corresponds to no signal. Clearly the DFWM signal is low-biased with most signal values being near zero while the DPCFWM histogram has a near Gaussian distribution around the mean. The reason for the poor signal quality in the case of DFWM can be traced to the beam-steering problem which becomes more and more important as the pressure increases. In fact, for DFWM the interaction volume is very different for each shot of the laser as observed when examining the data.

In order to determine a value for OH number density, a signal equation relating signal intensity, number density, molecular transition strength, linewidth, as well as other important parameters is required. An exact signal equation, however, is neither known nor established at this time. Also, the effects of pressure broadening and laser linewidth on signal strengths are not well known for DFWM or DPCFWM. Because of these complications, in our analysis we simply assume that the relation of Dreier et al. [4, 5] shown in (2) is correct for both DFWM and DPCFWM at elevated pressure. It is noted that in our experiment the laser linewidth is larger than the OH $Q_1(13)$ broadened line up to 9 bar, where it is believed these linewidths are equal.

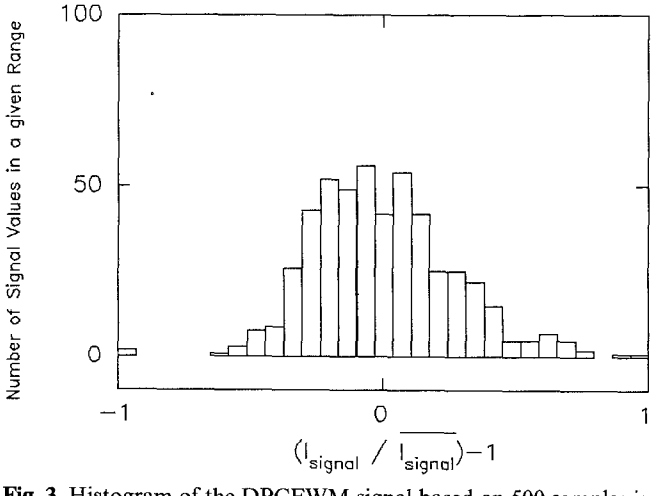

Fig. 3. Histogram of the DPCFWM signal based on 500 samples in the same lean methane/air laminar flame: $\phi=0.85$ at 9 bar and 5 mm above the burner

After making these assumptions absolute values of OH number density can be determined based on (2) relative to a reference condition. In our measurements we select a reference condition 5 mm above the burner in a stoichiometric, $\phi=1.0$, premixed, flat, laminar, methane/air flame at 1 bar. The OH number density at this condition has been measured several times over a three year period using direct absorption to be 7.0×10^{15} molecules/cm^3 [12, 18]. Based on this reference value the absolute values of OH number density of the 1, 5, and 9 bar, $\phi=0.85$, flames have been determined and are summarized in Table 3 for the two optical-path laser-induced fluorescence [12, 18] (TOPLIF), DFWM, and DPCFWM techniques. At 1 bar the agreement between the three techniques is good. At 5 and 9 bar the agreement between the TOPLIF and DPCFWM values is good; however, for the DFWM technique the OH number density is lower than for both TOPLIF and DPCFWM. This discrepancy can be explained by examining the histograms shown in Figs. 2, 3 where it is noted that DFWM is a non-Gaussian, in fact nearly log-normal, at 9 bar, low-biased histogram.

Rotational temperatures at 5 and 9 bar have been determined by making DPCFWM spectral scans of the R_1 and R_2 branches of the OH molecule in the $A^2\Pi(v'=0)\Leftarrow X^2\Sigma^+(v''=0)$ electronic system (Figs. 4, 5, respectively). Following the analysis of Dreier et al. [4, 5] the signal intensity is given by the expression

$$I_{Signal}\approx[B_{ij}N_{OH}(v'',j'')]^2\,, \tag{2}$$

where $N_{OH}(v'', j'')$ is the rotational state-specific number density and B_{ij} the one-photon line strength of the molecular transition [14]. Assuming a Boltzmann distribution of the rotational levels

$$N_N(v=0)\approx(2J+1)\exp(-\Delta E_N hc/kT)\,, \tag{3}$$

Table 3. Comparison of absolute values by method of OH number density in molecule/cm^3 at 1, 5, and 9 bar, 5 mm above burner, $\phi=0.85$

Pressure [bar]	TOPLIF [12]	DFWM	DPCFWM
1.0	8.0×10^{15}	9.0×10^{15}	9.5×10^{15}
5.0	9.0×10^{15}	7.0×10^{15}	9.0×10^{15}
9.0	14.0×10^{15}	6.5×10^{15}	12.5×10^{15}

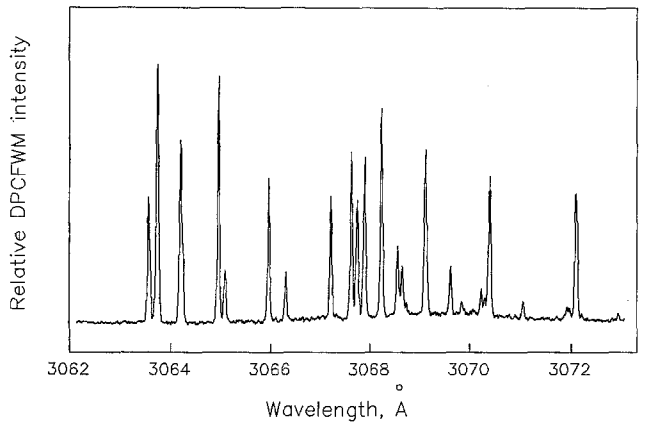

Fig. 4. DPCFWM spectra of OH R_1 and R_2 branches of the $A^2\Pi(v'=0) \Leftarrow X^2\Sigma^+(v''=0)$ system detected in the 5 bar; $\phi = 0.85$ methane/air flame at 5 mm

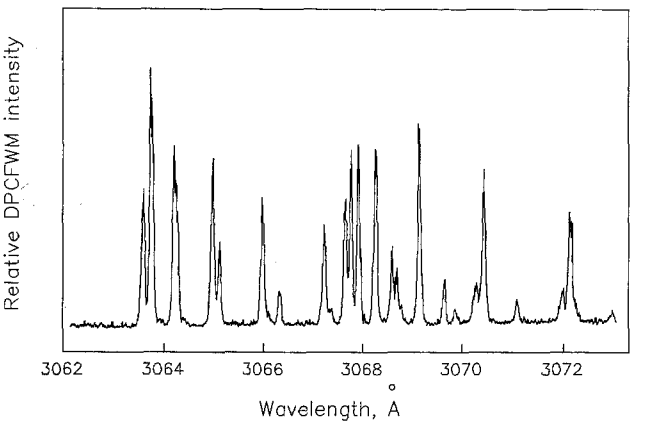

Fig. 5. DPCFWM spectra of OH R_1 and R_2 branches of the $A^2\Pi(v'=0) \Leftarrow X^2\Sigma^+(v''=0)$ system detected in the 9 bar; $\phi = 0.85$ methane/air flame at 5 mm

where ΔE_N is the term value of the rotational level $J = N \pm 1/2$ and h, c, k, and T have their usual meaning. A plot of

$$\ln\left(\frac{\sqrt{I_{\text{signal}}}}{(2J+1)B_{ij}}\right) \tag{4}$$

versus rotational energy, ΔE_N, should give a straight line whose slope is directly equal to $-1/T_{rot}$.

Such a Boltzmann plot of the OH population derived from the DPCFWM spectra at 5 bar (Fig. 6) and at 9 bar (Fig. 7) have been constructed from the DPCFWM spectra shown in Figs. 4 and 5, respectively. The rotational temperatures in the premixed methane/air flame, $\phi = 0.85$, have been determined to be 1910 K $\pm$ 150 K at 5 bar and 1940 K $\pm$ 150 K at 9 bar. These temperatures agree well with previous [12] fluorescence measurements and computations in the same flame using the STANJAN chemical equilibrium code where it was determined that these temperatures are between 1800 K and 1900 K in the same flame for $\phi = 0.85$ for both 5 bar and 9 bar. It is known that the temperature is lower than the adiabatic flame temperature, 2068 K for $\phi = 0.85$ at 5 bar, and 2079 K for $\phi = 0.85$ at 9 bar, because of the heat losses at the burner surface and radiation losses. The accuracy of the temperature measurements, $\pm$150 K, based on the Boltzmann plots has been conservatively estimated from independent spectral scans of the R_1 and R_2 branches and noting the variations. In order to achieve greater confidence in the temperature measurement, the following points should be pursued; 1) Use of a monomode laser to minimize shot by shot spectral instabilities underneath the laser bandwidth and, 2) Study the effects of saturation, collisional quenching, power and pressure broadening, and atomic motion, which are not fully understood at the present.

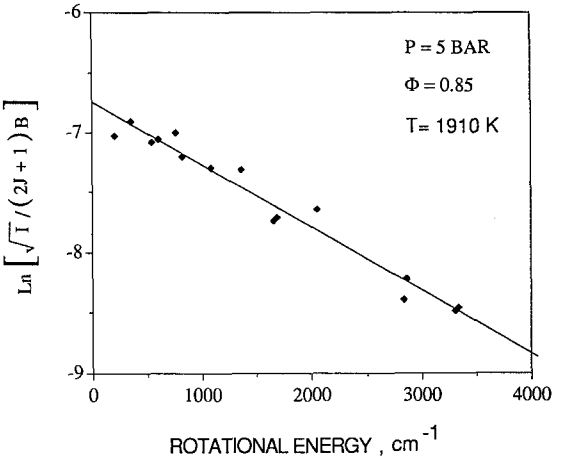

Fig. 6. Boltzmann plot of the population density from the DPCFWM spectrum shown in Fig. 4 at 5 bar. From the slope of linear least-squares fit through the data points an OH rotational temperature of 1910 K is found

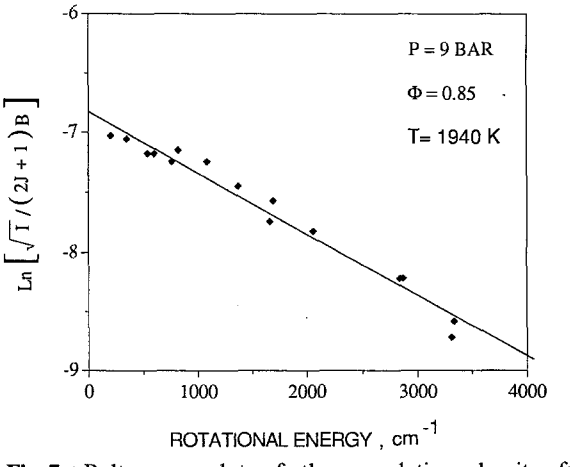

Fig. 7. Boltzmann plot of the population density from the DPCFWM spectrum shown in Fig. 5 at 9 bar. From the slope of linear least-squares fit through the data points an OH rotational temperature of 1910 K is found

3 Conclusion

The present results demonstrate the effectiveness of the DPCFWM technique to measure 1) OH number density

and 2) rotational temperatures in laboratory flames up to 9 bar. The application of a phase-conjugate backward pump to the forward pump enables one to make accurate measurements at higher pressures than atmospheric. However, at atmospheric pressure the conventional DFWM technique in our experimental setup is slightly more stable than the DPCFWM method. This may not be the same for every experiment since the magnitude of the temperature gradients and laser bandwidth, for example, vary from one experiment to the other. It is also known that as the pressure increases the beam-steering effects become more and more severe, and the phase-conjugate property of the backward pump in the DPCFWM technique enables one to maintain a near constant interaction volume. At atmospheric pressure fluctuations in the DFWM signal are somewhat less than for DPCFWM. However, at 5 and 9 bar the DFWM signals are low-biased due to a non-constant forward pump, backward pump, and probe interaction volume. At pressures higher than atmospheric the DPCFWM is a technique which makes quantitative measurements possible.

Future efforts in our laboratory will be: 1) to study experimentally DPCFWM linewidth, line shape, and saturation effects, and 2) to use the DPCFWM method in a two-dimensional configuration.

Acknowledgements. The authors wish to acknowledge the financial support of the CNRS-PIRSEM and ELF-Aquitaine. The technical assistance of Dr. Frédéric Dionnet in connection with the Lecroy Data Acquisition system is also gratefully acknowledged.

References

1. M. Winter, P.P. Radi: Opt. Lett. **17**, 320–322 (1992)
2. M. Winter, P.P. Radi, A. Stampanoni: 24th Int'l Symp. on Combustion (The Combustion Institute, Pittsburgh 1992)
3. J. Pender, L. Hesselink: Opt. Lett. **10**, 264–266 (1985)
4. T. Dreier, D.J. Rakestraw: Appl. Phys. B **50**, 479–485 (1990)
5. T. Dreier, D.J. Rakestraw: Opt. Lett. **15**, 72–74 (1990)
6. P. Ewart, S.V. O'Leary: Opt. Lett. **11**, 279–281 (1986)
7. P. Ewart, P. Snowdon, I. Magnusson: Opt. Lett. **14**, 563–565 (1989)
8. H. Bervas, B. Attal-Trétout, S. Le Boiteux, J.P. Taran: J. Phys. B: At. Mol. Opt. Phys. **25**, 949–969 (1992)
9. D.J. Rakestraw, R.L. Farrow, T. Dreier: Opt. Lett. **15**, 709–711 (1990)
10. D.J. Rakestraw, L.R. Thorne, T. Dreier: 23rd Int'l Symp. on Combustion (The Combustion Institute, Pittsburgh 1990) pp. 1901–1907
11. B. Attal-Trétout, S.C. Schmidt, E. Crété, P. Dumas, J.P. Taran: J. Quant. Spectrosc. Radiat. Transfer **43**, 351–364 (1990)
12. P. Desgroux, E. Domingues, D.A. Feikema, A. Garo, M.-J. Cotterau: 13th Int'l Colloquium on Dynamics of Explosions and Reactive Systems, Nagoya, Japan (1991)
13. R.L. Abrams, J.F. Lam, R.C. Lind, D.G. Steel, P.F. Liao: *Optical Phase Conjugation*, ed. by R.A. Fisher (Academic, New York 1983) pp. 211–284
14. I.L. Chidsey, D.R. Crosley: J. Quant. Spectrosc. Radiat. Transf. **23**, 187–199 (1980)
15. A. Yarif: *Quantum Electronics*, 3rd edn. (Wiley, New York 1988) pp. 475–506
16. R.C. Weast, M.J. Astle, W.H. Beyer: 64th edn., CRC Handbook of Chemistry and Physics (CRC, Boca Raton, FL 1984)
17. K. Kohse-Höinghaus, U. Meier, B. Attal-Trétout: Appl. Opt. **29**, 1560–1569 (1990)
18. P. Desgroux, E. Domingues, M.-J. Cottereau: Appl. Opt. **31**, 2831–2838 (1992)